

Lawrence Berkeley National Laboratory

Advanced Light Source

Title

Cerium oxide nanoparticles transformation at the root-soil interface of barley (*Hordeum vulgare* L.)

Permalink

<https://escholarship.org/uc/item/01w5n579>

Journal

Environmental Science Nano, 5(8)

ISSN

2051-8153

Authors

Rico, Cyren M
Johnson, Mark G
Marcus, Matthew A

Publication Date

2018-06-01

DOI

10.1039/c8en00316e

Peer reviewed



EPA Public Access

Author manuscript

Environ Sci Nano. Author manuscript; available in PMC 2022 September 23.

About author manuscripts

Submit a manuscript

Published in final edited form as:

Environ Sci Nano. 2018 June ; 5(8): 1807–1812. doi:10.1039/C8EN00316E.

Cerium oxide nanoparticles transformation at the root-soil interface of barley (*Hordeum vulgare* L.)

Cyren M. Rico^{1,2,4,*†}, Mark G. Johnson², Matthew A. Marcus³

¹National Research Council, Research Associateship Program, 500 Fifth Street, NW, Washington, DC 20001, USA

²US Environmental Protection Agency, National Health and Environmental Effects Research Laboratory, Western Ecology Division, 200 SW 35th St., Corvallis, OR 97333, USA

³Advanced Light Source, Lawrence Berkeley National Laboratory, 1 Cyclotron Road, Berkeley, CA 94720, USA

⁴Missouri State University, Department of Chemistry, 901 S National Ave., Springfield, MO 65897, USA

Abstract

The transformation of cerium oxide nanoparticles (CeO₂-NPs) in soil and its role in plant uptake is a critical knowledge gap in the literature. This study investigated the reduction and speciation of CeO₂-NPs in barley (*Hordeum vulgare* L.) cultivated in soil amended with 250 mg CeO₂-NPs kg⁻¹ soil. Synchrotron micro-X-ray fluorescence (μXRF) was employed for spatial localization and speciation of CeO₂-NPs in thin sections of intact roots at the soil-root interface. Results revealed that Ce was largely localized in soil and at the root surface in nanoparticulate form (84–89%). However, a few hot spots on root surfaces revealed highly significant reduction (55–98%) of CeO₂-NPs [Ce(IV)] to Ce(III) species. Interestingly, only roots in close proximity to hot spots showed Ce uptake which was largely CeO₂ (89–91%) with very little amount Ce(III) (9–10%). These results suggest that the reduction of CeO₂-NPs to Ce(III) is needed to facilitate uptake of Ce.

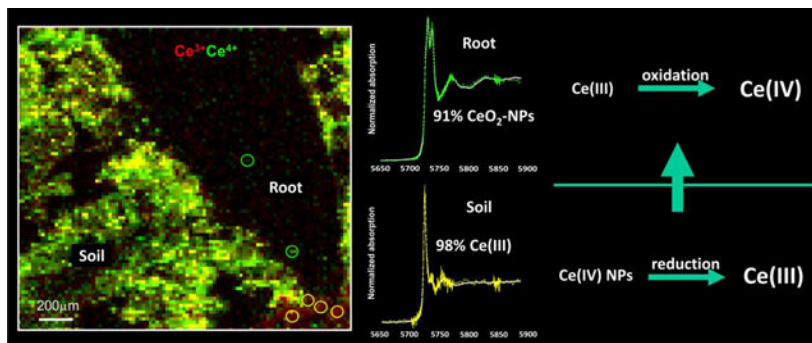
Graphical Abstract

*Corresponding author. Tel: 417 836 3304; Fax: 417 836 5507; CyrenRico@MissouriState.edu (C. M. Rico).

†This research was started at US EPA and finished at Missouri State University. Specifically, reference spectra for linear combination fit analysis were obtained when the first author moved to Missouri State University.

Supporting Information

Detailed description of methods, Yoshida nutrient solution composition, XRF map acquisition, speciation studies on CeO₂-NPs are available at <http://pubs.acs.org>.



Keywords

Nanoceria reduction; nanomaterials transformation; Synchrotron micro-X-ray fluorescence

INTRODUCTION

Cerium oxide nanoparticles (CeO₂-NPs) are highly stable nanoparticles that undergo very limited transformation in different environmental media.¹ However, recent studies^{2–9} using synchrotron spectroscopic techniques showed that plants could enhance CeO₂-NPs reduction [Ce(IV) → Ce(III)] to as much as 23% Ce(III) in soil,³ and 34% Ce(III) acetate, 22% Ce(III) carboxylates, 40% Ce(III) phosphate, 40% Ce(III) oxalate in hydroponic culture^{6,8} (Supporting Information (SI) Table 1). These enhanced transformations have been attributed to root exudates (i.e. reducing substances such as organic acids, cellulosic materials, amino acids) that plants release when exposed to CeO₂-NPs.^{6,8}

Previously, we showed peculiar differences on the uptake and translocation of Ce in rice, wheat and barley cultivated to full maturity in CeO₂-NPs amended soil: rice and barley accumulated Ce in plant tissues and grains, whereas wheat did not transport Ce to the aboveground tissues and grains.^{12–13} These plants were cultivated in similar growth conditions following soil exposure to CeO₂-NPs. Therefore, it could be inferred that the discrimination on Ce uptake could have occurred through the roots wherein chemical environment and nanoparticle behavior in the root-soil interface controlled the differences on plants' ability to transport Ce into the roots and aerial parts.

Recently, we reported a follow-up study to understand the transformation and uptake of CeO₂-NPs in wheat. Synchrotron micro X-ray fluorescence (μXRF) and micro X-ray absorption spectroscopy (μXAS) techniques revealed the limited transformation of CeO₂-NPs in full profile intact root-soil system with no evidence of plant uptake or accumulation;¹⁰ a finding that corroborated the results from our previous study in wheat.¹¹ In view of these findings, assessing the speciation of Ce in the root-soil system of barley exposed to CeO₂-NPs may yield information on how Ce is taken up by the roots and translocated to the grains in barley as opposed to being immobilized in wheat roots.

This study investigated the chemical fate of CeO₂-NPs in the rhizosphere of barley and its possible role on Ce accumulation inside the roots. Since Ce was detected in the aerial

parts of barley, it was hypothesized that the behavior (i.e. speciation, transformation) of CeO₂-NPs in the rhizosphere influenced the uptake of Ce in roots. Thus, this study focused on the speciation of CeO₂-NPs in root-soil interface using synchrotron spectroscopy.

MATERIALS AND METHODS

Preparation of plants and root thin sections for synchrotron analysis

This study is a continuation of research on long-term impacts of CeO₂-NPs in barley. The CeO₂-NPs (Meliorum Technologies, Rochester, NY) are rods with primary size of $(67 \pm 8) \times (8 \pm 1)$ nm (length \times diameter), particle size of 231 ± 16 nm in DI water, surface area of 93.8 m²/g, and 95.14% purity.¹⁴ The preparation of nanoparticle suspension and plant cultivation were described in previous studies and given in the SI.^{10–13} Briefly, barley seedlings were cultivated in soil for 60 days in growth chamber (Environmental Growth Chamber, Chagrin Falls, OH) with conditions maintained at 16-h photoperiod, 20/10°C, 70% humidity, 300 μ mol/m²-s for the first 40 days, after which the light intensity was increased to 600 μ mol/m²-s. One hundred mL of Yoshida nutrient solution¹⁵ (nutrient composition was provided in SI) was added to the pots on the day the seedlings were transplanted.

Samples for synchrotron analysis was prepared following the method described previously.^{10,16,17} Briefly, soil core was collected in a 2.5 cm \times 6 cm (diameter \times height) aluminum cylinder, wrapped in plastic, and kept frozen (–80°C). The cores were embedded with Spurr's Resin, cut in half along the long axis, and 3–5 cm by 7 cm glass slides were glued to the cut surface to cover the entire cut surface on one half of each core. Further processing (i.e. cutting and polishing) produced intact root/soil thin-sections with a thickness of ~100 μ m.

Localization and in situ speciation of Ce in intact root-soil system

The μ XRF mapping and μ XANES analysis of Ce at the L₃ edge in the barley root-soil thin sections was performed at 10.3.2 X-ray Microprobe Beamline at the Advanced Light Source (ALS) at Lawrence Berkeley National Laboratory following the method described in Rico et al.¹⁰ and given in the SI. μ XANES data for spots of interest as well as reference spectra were taken in fluorescence, using the QXAS flying-energy-scan mode of data acquisition.

Reference standard μ XANES spectra for linear combination fit (LCF) were obtained from Ce(IV) oxide nanoparticles, Ce(III) acetate, Ce(III) carbonate, Ce(III) oxalate, and Ce(III) phosphate.^{2,3,7} The standards were prepared by blending a 1:1 (w/w) ratio of the standards and boron carbide (B₄C) with a clean agate mortar and pestle. Small amounts of these mixtures were bound on Kapton tape and presented to the μ XRF beamline. The beam energy was calibrated so that the first peak for CeO₂-NPs was at 5730.39eV. Data were taken with a fine spacing near 5848.6eV, where a monochromator Bragg glitch served as an internal energy calibrant for each spectrum. The short dwell time in this region is the source of the noisiness of all spectra there. Because the white-line intensity is high, the fluorescence spectra for the Ce(III) references are very sensitive to overabsorption (“self-absorption”).^{18,19} Therefore, we took spectra at places where the intensity was high, for good signal, and at tiny particles, where the spectra were noisy but the same for a range

of particles which yielded different count rates. We thus considered that these particles were small enough to avoid overabsorption, and adjusted the spectra from the stronger-signal areas using a simple model for overabsorption with the amount of overabsorption varied so the spectral shapes for the strong-signal areas matched those for the tiny particles. This procedure gives us the signal quality from the strong-signal areas and the freedom from overabsorption found with small particles.

The μ XANES spectra from the reference compounds were presented in Figure 1. LCF values obtained were not significantly different from each other so that it was difficult to determine the preferred Ce(III) species. Thus, LCF from one Ce(III) species was used (SI Table 2).

RESULTS AND DISCUSSION

The μ XRF elemental maps from intact root-soil rhizosphere of treated barley revealed a heavy presence and wide distribution of Ce in soil. Figure 2A depicts the thin section of intact rhizosphere and the area (marked by the box) where elemental and chemical maps were acquired. The μ XRF maps indicate that Ce was mostly adsorbed on the barley roots or aggregated in the soil just outside the roots, but was not detected inside the roots (Figure 2B,C,D). This data is similar with our previous finding which showed high concentration of Ce on wheat root surface.¹⁰ Hernandez et al.⁴ also reported CeO₂-NPs adsorption in mesquite root grown in hydroponic culture.

Selected hotspots were interrogated for Ce speciation, and showed that Ce was mostly in oxide form in spots analyzed in roots 1, 2 and 3 (Figure 2B1,C1,D1, SI Table 2). LCF data showed that Ce was present mostly as CeO₂ (84–92%) with small amounts of Ce(III) species (9–15%). The μ XANES of CeO₂ has a distinct shoulder on the low-energy side not found in other Ce(IV) species, and this shoulder is seen in all our spectra for which the signal is good enough to see it.²⁰ We see no evidence for any Ce(IV) species other than CeO₂. On the other hand, the μ XANES of CeO₂-NP differs very little from that of bulk CeO₂, so we cannot distinguish bulk from nano and refer to both as CeO₂. This data demonstrates that CeO₂-NPs undergo very limited transformation in barley root-soil system, which is consistent with our findings in wheat rhizosphere that showed only 3–12% reduction to Ce(III) species.¹⁰ Previous studies also showed similar results in transformation of CeO₂-NPs to Ce(III) acetate, carboxylate, phosphate, and hydroxide in plants (SI Table 1).^{3,4,5,7,9}

We found Ce(III) signal near the tip of root 3, which indicates that a fraction of the CeO₂ [Ce(IV)] were reduced to Ce(III). A second chemical map of root 3 extending further down from the root tip was acquired at longer x-ray dwell time of 200 milliseconds (Figure 3). Remarkably, root 3 spots 7, 8, 9, and 10 showed reduction of CeO₂ to Ce(III) species by 61, 77%, 56%, and 98%, respectively (Figure 3E3-E6). μ XRF map also revealed CeO₂ inside barley root in the area close to where Ce(III) was detected (Figure 3E1,E2). Root 3 spots 5 and 6 revealed that Ce was 89–91% CeO₂ with small amount of Ce(III) species (9–10%) (Figure 3E1,E2). Based on this data, it is possible that Ce was taken up by barley roots as Ce(III), which got re-oxidized back to CeO₂ inside the roots. Schwabe et al.²¹ reported

that pumpkin and sunflower root exudates caused dissolution of CeO₂-NPs that potentially facilitated the root uptake of Ce(III). Perhaps barley also produced extracellular compounds that reduced Ce(IV) and resulted in Ce(III) uptake in roots.

This is the first time that large reduction of CeO₂-NPs to Ce(III) has been recorded in soil. The highest value we found in literature was 48% Ce(III) phosphate in soil, and 40% Ce(III) phosphate and 34% Ce(III) acetate in cucumber roots grown in hydroponic culture.^{4,6,8} As noted above, our previous study on wheat exposed to CeO₂-NPs at similar soil and growing conditions used in the current experiment only showed 3–12% reduction of CeO₂ to Ce(III) species.¹⁰ Barley might have different root exudates than those from soybean, wheat, and cucumber in other experiments.^{4,8,10} Related study shows that plant type significantly alters concentrations and compositions of root exudates in stressed plants (i.e. Pb-exposed *Sedum alfredii*).²²

The results also suggest that reduction sites for Ce may be highly localized since the huge amount of Ce(III) was observed in root 3 only. This is consistent with reports showing that root exudate (e.g. oxalate produced by plants) or oxidation-reduction sites tend to occur in isolated patches in roots.^{23,24} With regard to Ce(III) → CeO₂ [Ce(IV)] formation inside the roots, this finding is consistent with a report showing uptake of Ce(III) ions that precipitated as CeO₂-NPs in leaves.²¹ Current results are also in contrast with our findings in wheat wherein only CeO₂-NPs, and no Ce(III), were detected in rhizosphere, and no Ce was found inside the roots.¹⁰ Both findings in wheat and barley corroborate our previous studies wherein aboveground accumulation of Ce was recorded in barley but not in wheat.^{10–12}

In summary, μXAS synchrotron spectroscopy revealed root surface adsorption and soil agglomeration of CeO₂-NPs with transformation of Ce(IV) → Ce(III) being highly localized in some roots. The study revealed up to 98% reduction of CeO₂-NPs to Ce(III) species in soil-root interface which potentially facilitates root uptake of Ce(III) species. CeO₂ were found inside roots which suggests Ce(III) oxidation to Ce(IV) once Ce(III) has moved into the plant. These results provide additional insights into the mechanism of Ce transport and accumulation in plants.

Supplementary Material

Refer to Web version on PubMed Central for supplementary material.

Acknowledgments

This work has been subjected to the EPA's peer and administrative review, and it has been approved for publication as a U.S. Environmental Protection Agency document. Mention of trade names or commercial products does not constitute endorsement or recommendation for use. The operations at the Advanced Light Source are supported by the Director, Office of Science, Office of Basic Energy Sciences, US Department of Energy under Contract No. DE-AC02-05CH11231.

References

1. Cornelis G; Ryan B; McLaughlin MJ; Kirby JK; Beak D; Chittleborough D. Solubility and batch retention of CeO₂ nanoparticles in soils. *Environ. Sci. Technol* 2011, 45, 2777–2782. [PubMed: 21405081]

2. Arai Y; Dahle JT Redox-ligand complexation controlled chemical fate of ceria nanoparticles in an agricultural soil. *J. Agric. Food Chem*, 2017, DOI: 10.1021/acs.jafc.7b01277.
3. Hernandez-Viezcas JA; Castillo-Michel H; Andrews JC; Cotte M; Rico C; Peralta-Videa JR; Ge Y; Priester JH; Holden PA; Gardea-Torresdey JL In situ synchrotron x-ray fluorescence mapping and speciation of CeO₂ and ZnO nanoparticles in soil cultivated soybean (*Glycine max*). *ACS Nano* 2013, 7, 1415–1423. [PubMed: 23320560]
4. Hernandez-Viezcas JA; Castillo-Michel H; Peralta-Videa JR; Gardea-Torresdey JL Interactions between CeO₂ nanoparticles and the desert plant mesquite: A spectroscopy approach. *ACS Sustain Chem. Eng* 2016, 4, 1187.
5. Majumdar S; Peralta-Videa JR; Bandyopadhyay S; Castillo-Michel H; Hernandez-Viezcas JA; Sahi S; Gardea-Torresdey JL Exposure of cerium oxide nanoparticles to kidney beans shows disturbance in the plant defense mechanisms. *J. Hazard. Mater* 2014, 278, 279–287. [PubMed: 24981679]
6. Zhang P; Ma Y; Zhang Z; He X; Zhang J; Guo Z; Tai R; Zhao Y; Chai Z. Biotransformation of ceria nanoparticles in cucumber plants. *ACS Nano* 2012, 6, 9943–9950. [PubMed: 23098040]
7. Zhang P; Ma Y; Liu S; Wang G; Zhang J; He X; Zhang J; Rui Y; Zhang Z. Phytotoxicity, uptake and transformation of nano-CeO₂ in sand cultured romaine lettuce. *Environ. Pollut* 2016, 20, 1400–1408.
8. Zhang P; Xie C; Ma Y; He X; Zhang Z; Ding Y; Zheng L; Zhang J. Shape-dependent transformation and translocation of ceria nanoparticles in cucumber plants. *Environ. Sci. Tech. Let*, 2017, 4, 380–385.
9. Spielman-Sun E; Lombi E; Donner E; Howard D; Unrine JM; Lowry GV Impact of surface charge on cerium oxide nanoparticle uptake and translocation by wheat (*Triticum aestivum*). *Environ. Sci. Technol* 2017, 51, 7361–7368. [PubMed: 28575574]
10. Rico CM; Johnson MG; Marcus MA; Andersen CP Intergenerational responses of wheat (*Triticum aestivum* L.) to cerium oxide nanoparticles exposure. *Environ. Sci.: Nano* 2017, 4, 700–711. [PubMed: 30147938]
11. Rico CM; Lee SC; Rubenecia R; Mukherjee A; Hong J; Perata-Videa JR; Gardea-Torresdey JL Cerium oxide nanoparticles impact yield and modify nutritional parameters in wheat (*Triticum aestivum* L.). *J. Agric. Food Chem* 2014, 62, 9669–9675. [PubMed: 25220448]
12. Rico CM; Barrios AC; Tan W; Rubenecia R; Lee SC; Varela-Ramirez AJ; Perata-Videa JR; Gardea-Torresdey JL Physiological and biochemical response of soil-grown barley (*Hordeum vulgare* L.) to cerium oxide nanoparticles. *Environ. Sci. Pollut. Res*, 2015, 22, 10551–10558.
13. Rico CM; Morales MI; Barrios AC; McCreary R; Hong J; Lee WY; Nunez J; Peralta-Videa JR; Gardea-Torresdey JL Effect of cerium oxide nanoparticles on the quality of rice (*Oryza sativa* L.) grains. *J. Agric. Food Chem* 2013, 61, 11278–11285. [PubMed: 24188281]
14. Keller AA; Wang H; Zhou D; Lenihan HS; Cherr G; Cardinale BJ; Miller R; Ji Z. Stability and Aggregation of Metal Oxide Nanoparticles in Natural Aqueous Media. *Environ. Sci. Technol* 2010, 34, 1962–1967.
15. Yoshida S; Forno DA; Cock JH; Gomez KA Laboratory Manual for Physiological Studies of Rice; International Rice Research Institute: Los Baños, Laguna, Philippines, 1976.
16. Langner P; Mikutta C; Suess E; Marcus MA; Kretzschmar R. Spatial distribution and speciation of arsenic in peat studied with microfocussed x-ray fluorescence spectrometry and x-ray absorption spectroscopy. *Environ. Sci. Technol* 2013, 47, 9706. [PubMed: 23889036]
17. Yamaguchi N; Ohkura T; Takahashi Y; Maejima Y; Arao T. Arsenic distribution and speciation near rice roots influenced iron plaques and redox conditions of the soil matrix. *Environ. Sci. Technol* 2014, 48, 1549. [PubMed: 24384039]
18. Goulon J; Goulon-Ginet C; Cortes R; Dubois JM On experimental attenuation factors of the amplitude of the EXAFS oscillations in absorption, reflectivity and luminescence measurements. *J. Phys* 1981, 42, 539–548.
19. Manceau A; Marcus MA; Tamura N. (2002) “Quantitative speciation of heavy metals in soils and sediments by synchrotron X-ray techniques”, in *Applications of Synchrotron Radiation in Low-Temperature Geochemistry and Environmental Science*, Fenter P. and Sturchio NC, Eds. *Reviews in Mineralogy and Geochemistry*, Mineralogical Society of America, Washington, DC., 49, 341–428.

20. Takahashi Y; Sakami H; Nomura M. Determination of the oxidation state of cerium in rocks by Ce L III-edge x-ray absorption near-edge structure spectroscopy. *Anal. Chim. Acta* 2002, 468, 345–354.
21. Schwabe F; Tanner S; Schulin R; Rotzetter A; Stark W; von Quadt A; Nowack B. Dissolved cerium contributes to uptake of Ce in the presence of differently sized CeO₂-nanoparticles by three crop plants. *Metallomics* 2015, 7, 466–477. [PubMed: 25634091]
22. Luo Q; Wang S; Sun LN; Wang H. Metabolic profiling of root exudates from two ecotypes of *Sedum alfredii* treated with Pb base on GC-MS. *Sci. Rep* 2017, 7, 39878. [PubMed: 28051189]
23. Anstoetz M; Rose TJ Clark MW; Lee LH; Raymond CA; Vancov T. Novel applications for oxalate-phosphate amine metal-organic-frameworks (OPA-MOFs): Can an iron-based OPA-MOF be used as slow release fertilizer? *PLoSOne* 2015, DOI:10.1371/journal.pone.0144169
24. Echigo T; Kimata M. Crystal chemistry and genesis of organic minerals: A review of oxalate and polycyclic aromatic hydrocarbon minerals. *Can. Mineral* 2010, 48, 1329–1358.

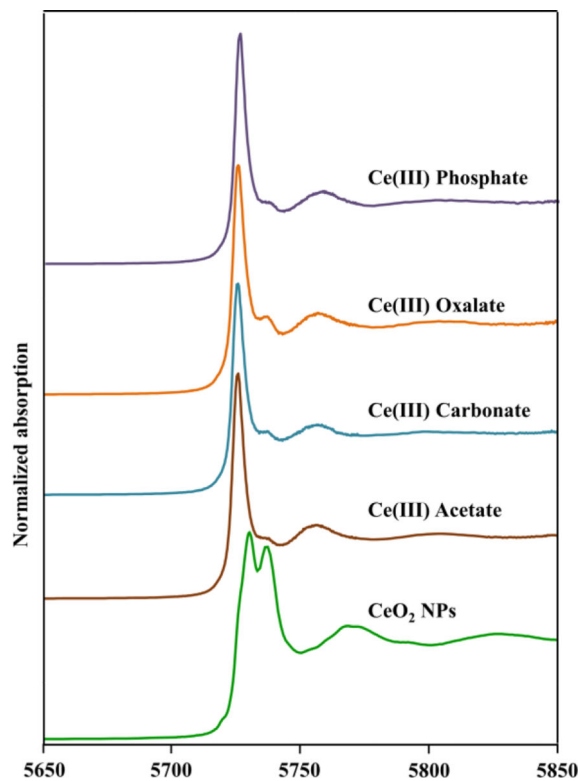


Figure 1. Ce μ XANES of the Ce model compounds. The shoulder seen in CeO₂ to the left of the first peak is not found in most other Ce(IV) compounds.

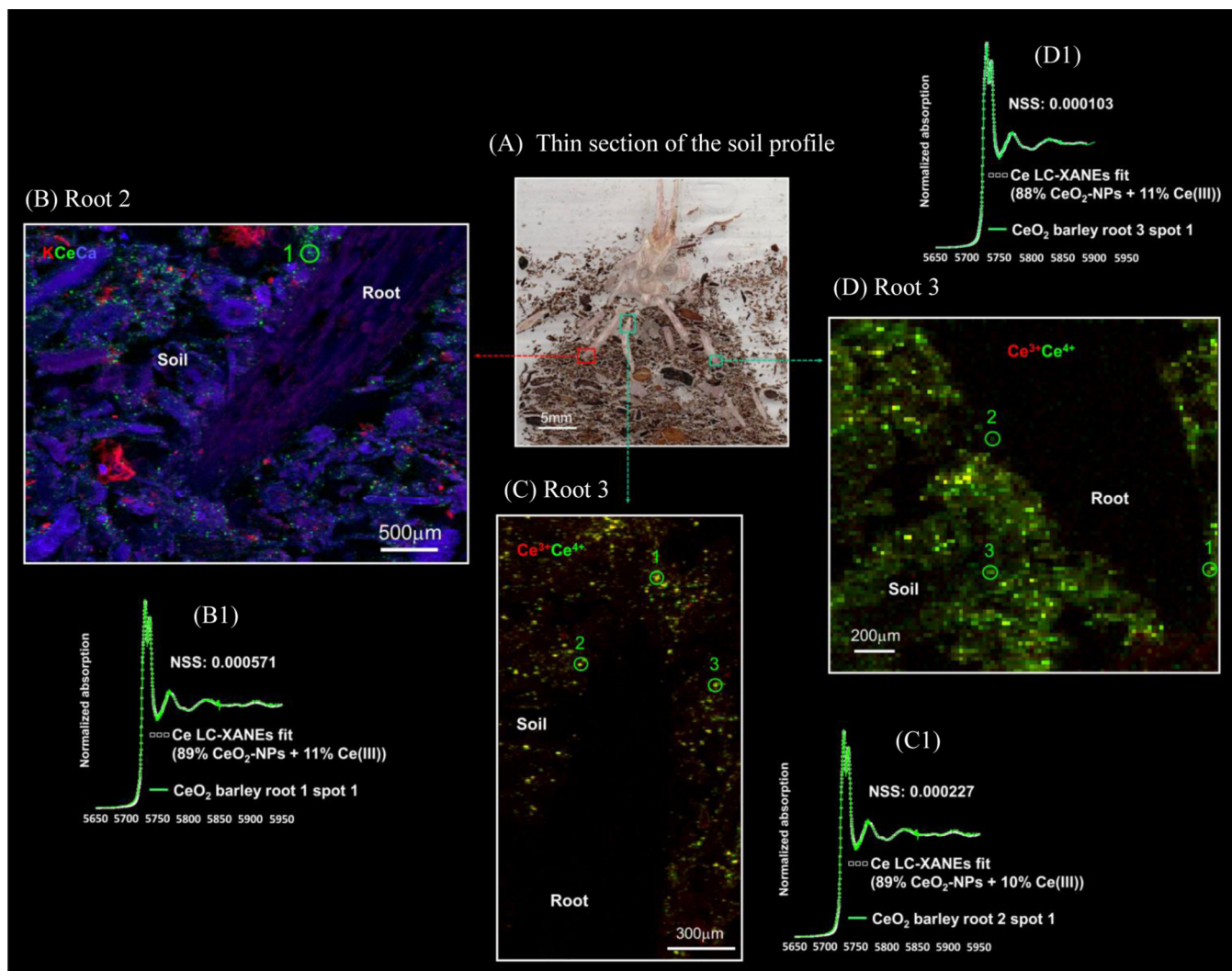


Figure 2.

Images of thin sections of soil profile from barley 60 days after treatment with 250 mg $\text{CeO}_2\text{-NPs kg}^{-1}$ soil. (A) Image showing intact root-soil rhizosphere. (B) tricolor μXRF chemical map of root 1 (red = K, green = Ce, blue = Ca). (C,D) Bicolor μXRF chemical map of roots 2 and 3 (red = Ce(III), green = Ce(IV)), respectively. (B1,C1,D1) Ce μXANES spectra from spots in root and soil. Spectra in green line represents μXANES from the sample, and white line represents linear combination (LC) fit. Proportions of $\text{CeO}_2\text{-NPs}$ and Ce(III) are values obtained from LC fits as provided in SI Table 2. μXRF mapping was performed with $20 \times 20 \mu\text{m}^2$ step size and 50 ms dwell time. NSS is normalized sum-square error of the fit.

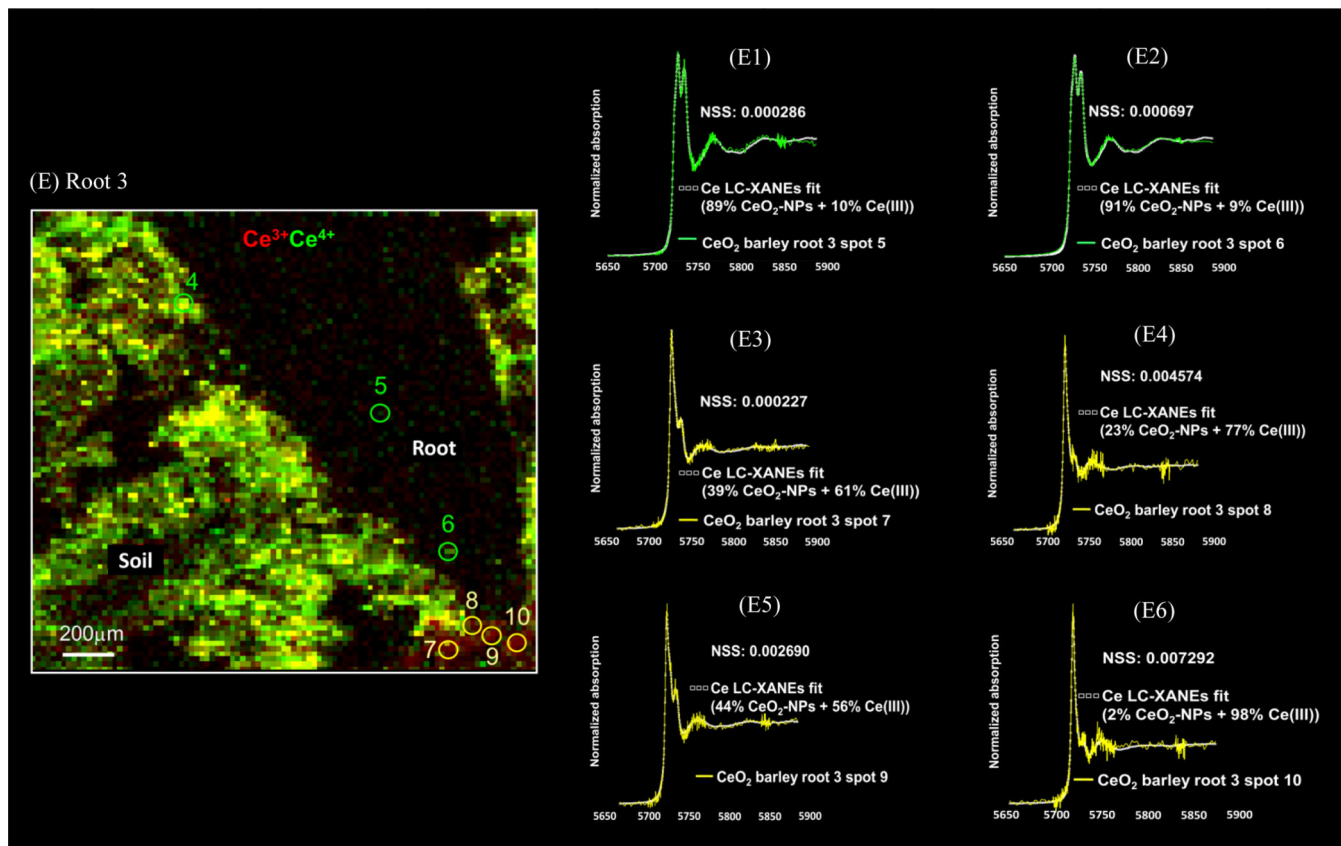


Figure 3.

(E) Bicolor μ XRF chemical map of root 3 (red = Ce(III), green = Ce(IV)). (E1,E2) Ce μ XANES spectra from spots 5 and 6, respectively. (E3,E4,E5,E6) μ XANES spectra from spots 7, 8, 9, and 10, respectively. Spectra in green or yellow line represents μ XANES from the sample, and white line represents linear combination (LC) fits. Proportions of CeO₂-NPs and Ce(III) are obtained from LC fits as given in SI Table 2. μ XRF mapping was performed with $20 \times 20 \mu\text{m}^2$ step size and 200 ms dwell time. NSS is normalized sum-square error of the fit.